Unveiling the Role of Hydrogen Bonds in Luminescent N-Annulated Perylene Liquid Crystals

Sergi Bujosa,[a] Elisa E. Greciano,[b] Manuel A. Martínez,[b] Luis Sánchez,*[b] and Bartolome Soberats*[a]

Abstract: We report the liquid-crystalline (LC) and luminescent properties of a series of N-annulated perylenes (1–4) in whose molecular structures amide and ester groups alternate. We found that the LC properties of these compounds not only depend on the number of hydrogen-bonding units, but also on the relative position of the amide linkers in the molecule. The absence of amide groups in compound 1 leads to no LC properties, whereas four amide groups induce the formation of a wide temperature range columnar hexagonal phase in compound 4. Remarkably, compound 3, with two amide groups in the inner part of the structure, stabilizes the columnar LC phases better than its structural isomer 2, with the amide groups in the outer part of the molecule. Similarly, we found that only compounds 1 and 2, which have no hydrogen bonding units in the inner part of the molecule, exhibit luminescence vapochromism upon exposure to organic solvent vapors.

Introduction

Discotic liquid crystals consist of extended π-conjugated scaffolds functionalized with flexible chains at the periphery, and generally self-organize through π-stacking of the aromatic moieties into columnar assemblies.[1] This assembly mode permits the overlap of the molecular orbitals of vicinal molecules enabling the excitonic coupling as well as charge carrier transport (hoping) along the 1D columns. Owing their optical and electronic properties, discotic liquid crystals are promising materials for photonics and organic electronics.[2] In early examples, the charge carrier properties of triphenylene derivatives exhibiting columnar phases were reported.[3] Discotic liquid crystals were shown later to be useful semiconductor materials in different electronic devices such as organic field effect transistors, solar cells and organic light emitting diodes.[1,2] Moreover, the discotic liquid crystals exhibiting fluorescence can be applied as smart systems exhibiting thermo- and/or mechanochromism.[4] Molecular engineering is key to control the materials properties, namely the excitonic coupling (J or H type), the thermal behavior and the charge carrier mobilities.[1–4] It is generally accepted that the size, shape and electron density of the core as well as the length, branching and polarity of lateral flexible chains are important parameters to control the properties of the materials.[5] Additionally, the introduction of functional groups prone to establishing additional noncovalent interactions, such as hydrogen bonds (H-bonds), have been shown to improve materials' performance, yielding more compact packing structures.[6] For example, Eichhorn and co-workers reported the introduction of hydrogen bonding (H-bonding) groups in tristhiophene tricarboxamide liquid columnar crystals exhibiting improved charge transport.[7] In the same direction, Kato and co-workers demonstrated the relevance of H-bonding in the development of mechanochromic liquid-crystalline (LC) materials based on dendronized π-conjugated cores (pyrene, anthracene, etc.).[4,8] In particular, H-bonds are able to stabilize metastable states (induced by mechanical shearing) with different emission properties than the initial thermodynamic state. More recently, it has been shown that that the introduction of H-bonding imide or lactam groups in dendronized perylene bisimides (PBIs) and diketopyrrolopyrroles cores leads to the formation of unconventional LC assemblies with the dyes oriented parallel to the columnar axis.[9] These materials exhibit J- and H-type aggregates, respectively. Thus, it is noteworthy that H-bonds are highly important for the stabilization and tuning the properties of functional liquid crystals.

We recently focused our research on the self-assembly of N-annulated perylenes (NAPs) as a suitable platform for the development of photoactive and optoelectronic materials, paying especial attention to the relationship between molecular design and the assembly mode. For example, we reported on the self-assembly properties in solution of a series of NAP

[a] S. Bujosa, Dr. B. Soberats
     Department of Chemistry
     Universitat de les Illes Balears
     Cra. Valldemossa, Km. 7.5, 07122, Palma de Mallorca (Spain)
     E-mail: b.soberats@uib.es

[b] E. E. Greciano, M. A. Martínez, Prof. Dr. L. Sánchez
     Departamento de Química Orgánica
     Facultad de Ciencias Químicas
     Universidad Complutense de Madrid
     Ciudad Universitaria, s/n; 28040 Madrid (Spain)
     E-mail: lusamar@ucm.es

Chemistry–A European Journal

Full Paper
doi.org/10.1002/chem.202102446

Chemistry
Europe
European Chemical
Societies Publishing

dicarboxamides capable to efficiently form H-bonded supramolecular polymers and luminescent gels.[10] More recently, we have prepared a new series of NAPs (compounds 1–4 in Figure 1a) bearing two terminal wedge-shaped derivatives and a variable number of amide/ester groups, and we proved their ability to display pathway complexity in supramolecular polymerization and the ability of compound 4 to act as circularly polarized light emitter.[11] Whilst LC PBIs have been widely studied,[9b,12] only few examples of bay-annulated perylenes showing LC properties have been reported.[13] In one of these scarce examples, the electroluminescent properties of bay-annulated perylene tetraester liquid crystals have been reported.[13b] Remarkably, in contrast to the majority of PBIs liquid crystals,[12] it has been shown that bay-annulated perylene systems keep their luminescent properties in solid and gel state,[10,13] and therefore they are very attractive for the development of stimuli-responsive and optoelectronic materials.[2,4]

In this work, we investigate the LC and stimuli responsive features of the luminescent NAPs 1–4 (Figure 1a) and unveil a direct correlation between the number and the position of the amide functional groups and their properties. That is, whilst compound 1, lacking the amide functional groups, shows no LC behavior, compound 4, bearing four amide groups, forms a columnar hexagonal (Col$_h$) phase in a wide temperature range (0–237 °C). More importantly, we found that compound 3 (isotropic at 174 °C), with the amide group closer to the core, stabilizes the columnar LC phases better than its structural isomer 2 (isotropic at 108 °C), with the amide groups located at the outer position from the core (Figure 1b). This behavior has

been attributed to the role of the H-bonds in the more efficient fixation of the columnar structure when the H-bonding groups are closer to the discotic core. Additionally, we prove that NAPs 1–4 exhibit luminescent properties in solid state, while compounds 1 and 2, with no amide groups close to the core, also exhibit vapofluorochromic behavior when exposed to vapors of organic solvents (CHCl$_3$, hexane, THF and toluene). These findings reveal novel molecular design features relevant for the development of luminescent discotic liquid crystals with stimuli responsive properties.

Results and Discussion

In the course of our investigations and taking into account the previous results reported for referable NPAs 1–4 (Figure 1a),[11] we thought that this family of compounds may also exhibit LC behavior. In addition, the systematic structural modifications could contribute to establish a clear structure-property relationship. Compounds 1 and 4 contain four ester and four amide connections, respectively, while 2 and 3 combine two ester and two amide groups but at different positions (Figure 1a). Compounds 1–4 were prepared following previously described methodologies,[11,14] and were isolated as yellow-brown powders. Importantly, all the compounds exhibited fluorescence properties in solution and in solid state (see below).

The LC behavior of compounds 1–4 was initially investigated by polarizing optical microscope (POM; Figure 2a, b and Figures S1 and S2 in the Supporting Information) and differential scanning calorimetry (DSC; Figures 2d and S3–S5). All the NAPs showed LC columnar phases (Figure 2c) except for compound 1, that shows a crystalline phase up to 44 °C, when melts to isotropic and decomposes as it can be deduced from the DSC curve (Figure S3) and the POM observations. All the other compounds show LC phases according to the POM observations. Figure 2a and b shows the POM images at 100 °C of compounds 2 and 3, respectively, which clearly show, under cross polarizers, birefringent textures that were found to correspond to columnar LC phases according to the X-ray experiments (see below). Compound 2 shows a single Col$_h$ phase from 55 to 108 °C, when clears. Curiously, both compounds 1 and 2, bearing ester groups directly linked to the NAP moiety, decompose when melting, suggesting the thermal weakness of this connection. In contrast, DSC of 3 (Figure 2d) reveals two enantiotropic LC (columnar) phases, the first one from 38 to 135 °C and the second from 135 to 174 °C. Compound 4, with two amide groups per peripheral branch, shows a single LC phase from 0 to 237 °C and the highest clearing point of the series (Figure 2c). These results are diagnostic of the stabilizing effect exerted by the amide groups of the NAP structure in the LC phases. However, the most striking results are found for the structural isomers 2 and 3. NAP 3, with the amide groups attached to the inner part of the molecule, shows a much higher melting temperature than 2, with the amide groups in the outer part of the linker. In particular, the melting temperature of 3 is 64 °C higher than that of 2. This observation indicates that not only the number of amide groups has relevant effects on the LC behavior
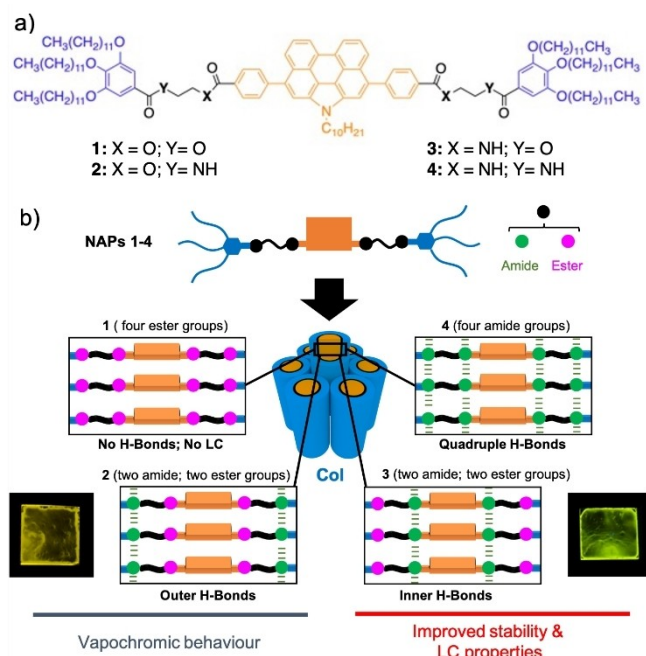

Figure 1. a) Molecular structure of NAPs 1–4. b) Schematic representation of the self-assembly features of compounds 1–4 and the proposed molecular interactions in the columnar phases. Insets show the luminescent films of compounds 2 (left) and 3 (right). The representation of the columnar packing of the NAPs in the side-view has been simplified for clarity.
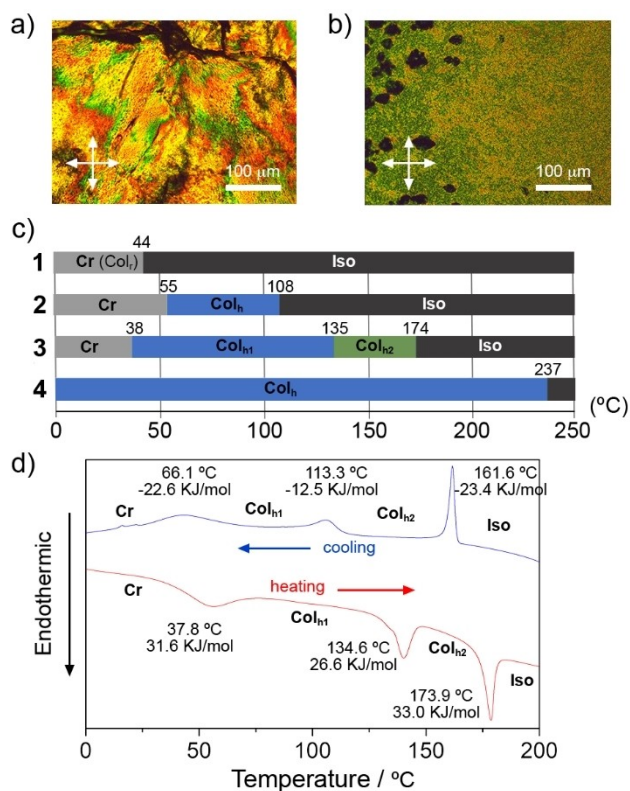
Chemistry–A European Journal

Full Paper
doi.org/10.1002/chem.202102446

Chemistry Europe
European Chemical
Societies Publishing

Figure 2. Polarizing optical microscope images of compounds a) **2** and b) **3** at 100 °C. c) Temperature-dependent phase-transition behavior of compounds **1–4**. Phase-transition temperatures were obtained from the first (**1** and **2**) and second (**3** and **4**) heating of the DSC curves. d) Second heating and first cooling DSC curves for compound **3**. Heating/cooling rate was 10 °C/min. Displayed transition temperatures correspond to the onset of the DSC peak.

of the NAP series, but also the position of these groups. Up to our knowledge, this observation has not been reported so far.

To figure out the organization of the phases displayed by **1–4**, we carried out X-ray-scattering (XRS) experiments. Unfortunately, we were unable to align the samples into fibers and perform anisotropic 2D X-ray experiments, relying therefore on 1D powder XRS experiments on polydomain samples (Figures 3
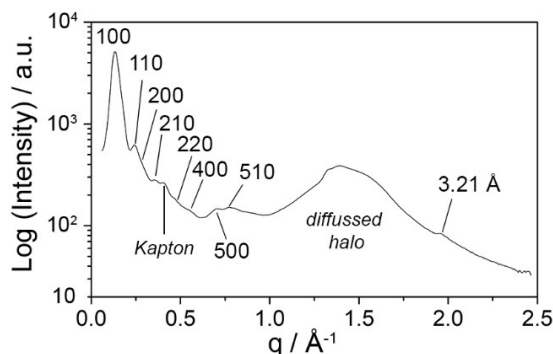

Figure 3. X-ray pattern of compound **2** at 100 °C. The pattern corresponds to a LC Col$_h$ phase ($a = 52.4$ Å).

and S6–S9). Compound **1** exhibits a crystalline columnar rectangular (Col$_r$) phase (Figure S6) up to 44 °C, when the compound decomposes. In contrast, the XRS pattern of compound **2** at 100 °C displays one intense peak at 45.4 Å and seven weaker peaks at 23.4, 22.4, 17.4, 13.4 11.5, 9.0 and 8.1 Å that were assigned to the 100, 110, 200, 210, 220, 400, 500 and 510 reflections of a Col$_h$ phase with an intercolumnar distance (a) of 52.4 Å (Figure 3). A diffuse halo, originated by the flexible alkyl chains, is also observed at 4.4 Å. On the other hand, compound **3** exhibits two distinct Col$_h$ phases, a lower temperature phase (Col$_{h1}$) with an $a = 50.4$ Å (100 °C) and a higher temperature phase (Col$_{h2}$) with an $a = 53.4$ Å (150 °C). Compound **4** exhibits also a Col$_h$ phase, whose intercolumnar distance (a) was found to be 55.4 Å at 150 °C (Figure S9).

By careful analysis of the XRS patterns, we observed that all the samples, except **1**, exhibit a small and sharp peak around 3.2–3.5 Å. This reflection was associated to the repeating distances along the z-axis ($00\,l$) of the 3D columnar lattice ascribable to π-π stacking distances. According to this, we can assume that the NAP molecules stack into columnar assemblies with the cores in the center of the columnar sections and the alkyl chains in the periphery (Figure 1b), like common discotic liquid crystals.[1] It is worth mentioning that compounds **2** and **3** show abnormally short π-π stacking distances, around 3.2 Å at 100 °C, which increase by heating the samples. These short π-π stacking distances can be rationalized by the strong interactions between the cores, probably enhanced by dipolar interactions. Table 1 displays the lattice parameters for all the LC phases of compounds **2–4** and the calculated number of molecules per layer (Z; see the Supporting Information).[9] Surprisingly, all the LC Col$_h$ phases of compounds **2–4** are composed of two molecules per columnar slice (3.2–3.5 Å). According to this, we propose a packing structure where in plane side-to-side dimers of perylene molecules stack forming columns (Figure S10) with the perylene core in the center and the alkyl chains (*N*-decyl and 3,4,5-trisdodecyloxybenzene) pointing outwards. This assembly mode is consistent with the columnar parameters obtained from the XRS experiments (Table 1) as well as with the molecular length of the NAPs (Figure S11).

To get more details about the role of H-Bonds in the stabilization of the LC phases, we performed FTIR experiments (Figure S12) for NAPs **1–4** at room temperature. Tetraester **1** shows the typical C=O ester stretching band at 1720 cm⁻¹ while compound **2** shows additionally the C=O amide stretching

Table 1. Lattice parameters for the columnar LC phases of NAPs **2–4**.

Comp.	T [°C]	LC phase	a [Å][a]	c [Å][a]	Z[b]
2	100	Col$_h$	52.4	3.21	2
3	100	Col$_{h1}$	50.4	3.23	2
3	150	Col$_{h2}$	53.4	3.32	2
4	150	Col$_h$	55.4	3.48	2

[a] All the values were obtained from the X-ray experiments. Parameter c corresponds to the π-stacking distance; [b] Z indicates the number of molecules per columnar cross-section and was calculated from the lattice parameters supposing a density of 0.9–1 g cm⁻³ (see the Supporting Information). The value provided (Z) corresponds to the whole number closer to the calculated value.

Chemistry–A European Journal

Full Paper
doi.org/10.1002/chem.202102446

Chemistry Europe
European Chemical
Societies Publishing

band at 1633 cm^{-1} and the N–H stretching band at 3271 cm^{-1}. The wavenumber of the NH stretching signals (<3400 cm^{-1}) are diagnostic of H-bonds.[11,15] Compounds **3** and **4** show the amide I C=O stretching band at ~1630 cm^{-1}, while also exhibiting two N–H stretching bands at ~3280 and ~3330 cm^{-1}. While the former band matches well with an intermolecular H-bond signal, the latter could be indicative of the residual presence of intramolecularly H-bonded seven-membered pseudocycles, as reported previously.[11b,d] Overall, the FTIR spectra of compounds **2**–**4** confirms the presence of H-bonding interactions in solid state, in accordance with the previous studies in solution.[11]

The photoactive properties of NAPs **1**–**4** were further studied in solution and in solid state. All the compounds exhibit an absorption band with a maximum at around 455–457 nm and an intense emission band with maximum at 479–487 nm in CHCl$_3$ solution (Figures S13–S16), which is consistent with the spectroscopic profile of the perylenes in the monomeric form.[11,14] For the solid-state experiments, the appropriate NAP solution (1 mg/mL, CHCl$_3$) was drop-casted onto quartz substrate and the sample was annealed at 40 °C for 4 h prior to perform the measurements. In good agreement with the previous results reported for the corresponding supramolecular polymers, the UV-Vis spectra in solid state of compounds **2**–**4** are consistent with the NAPs forming H-type aggregates (Figures S14–S16).[11] However, the UV-Vis spectrum of tetraester **1** in solid state exhibits a monomer-like absorption profile, which is an indication of a poor coupling among the monomeric units, in good accord with that previously reported in solution (Figure S13). Interestingly, we observed two distinct solid-state emission patterns for the series of NAPs. While compounds **1** and **2** exhibit a unimodal emission band with a maximum at 530–537 nm, the fluorescence spectra of compounds **3** and **4** show two maximums at 544–547 and 516–519 nm (Figures 4a, S15 and S16). These differences in the emission spectra can be appreciated by naked eye as shown in Figure 4b. Thin films of compounds **3** and **4** are green under a UV lamp (365 nm) exposure, while the films of **1** and **2** show yellow emission. This yellow emission is consistent with the formation of partial excimers, according to the unimodal profile of the emission spectra[4,8] (Figures 4a, S13, and S14) and the short π–π distances observed in the X-ray experiments (Table 1).

Then, we examined the changes in the photophysical properties of the NAPs **1**–**4** thin films upon application of different stimuli. No significant color changes were observed by application of mechanical force (shearing).[4,8,16] However, the thin films of **1** and **2** exhibited the reversible emission change upon exposure to vapors of organic solvents such as CHCl$_3$, THF, hexane or toluene (Figures 4c and S17–S19),[17,18] while thin films of **3** and **4** showed no significant changes (Figures S20 and S21). In particular, the thin film of **2** shows (under exposure to 365 nm light) an enhancement of the emission and a concomitant color change from yellow to green when exposed to CHCl$_3$ vapors (Figure 4c). This change is very quick (<4 s), and the film rapidly returns (<2 seconds) to the original state when ventilated with air. The repeatability of the sensing system was tested by subjecting the films of **1** and **2** to 10 exposition–venting cycles (CHCl$_3$-air), and we observed no degradation of the films and a reproducible color change (yellow→
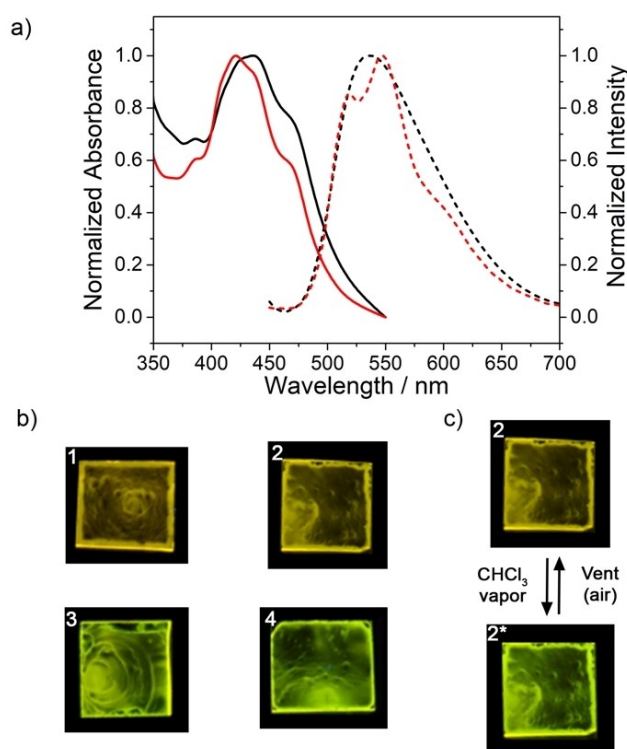

Figure 4. a) Normalized absorption (solid lines) and emission spectra (dashed lines) of drop-cast samples of **2** (black) and **3** (red) onto quartz plates. b) Photographs of the films of **1**–**4** on glass plates upon 365 nm irradiation. c) Image of an illuminated (365 nm) thin film of **2** under air conditions (top) and exposed to CHCl$_3$ vapor (bottom).

green→yellow) during all the cycles. We hypothesized that this color change occurs due to displacements between the NAP cores in within the columnar assembly induced by the diffusion of the organic molecules within the LC arrays. These displacements induce the disruption of the partial excimers and the concomitant yellow to green emission shift. Accordingly, seems that the key factors for the vapochromism in **1** and **2** are i) the formation of partial excimers in the LC columnar phases, and ii) an appropriate rotational and translational freedom in the columnar stacks.

Conclusion

In this work, we have elucidated the liquid-crystalline properties of a series of N-annulated perylenes (**1**–**4**) whose molecular structures contain alternating amide and ester groups. We found that the liquid-crystalline behavior of these materials is strongly dependent on the number of amide groups present in the molecule: compound **1**, with four ester groups, shows no liquid-crystalline properties whereas compound **4**, with four amide groups, shows a liquid-crystalline columnar hexagonal phase over a wide temperature range. Importantly, through study of the structural isomers **2** and **3**, we demonstrated the importance of the position of the hydrogen bonds in stabilizing liquid-crystalline phases. While the columnar phase of **2**, with amide groups in the outer part of the molecule, melts at 108 °C,

Chemistry–A European Journal

Full Paper
doi.org/10.1002/chem.202102446

Chemistry Europe
European Chemical
Societies Publishing

compound **3**, with amide groups in the inner part of the molecule, exhibits liquid crystallinity up to 173 °C. We believe that this effect can be explained by a more efficient reduction in the rotational and translational motions at the center of the columnar phase when the H-bonds are closer to the core. Importantly, these findings have implications on the photophysical and stimuli-responsive properties of **1–4**. Similarly, we reveal that the vapochromic behavior of compounds **1** and **2** is precisely enabled by the absence of hydrogen bonds close to the perylene core. We believe that the conclusions found in this study are relevant for the design of novel discotic liquid crystals in order to obtain ample temperature range liquid-crystalline phases and desired stimuli-responsive properties.

Acknowledgements

Conflict of Interest

The authors declare no conflict of interest.

[1] a) T. Wohrle, I. Wurzbach, J. Kirres, A. Kostidou, N. Kapernaum, J. Litterscheidt, J. C. Haenle, P. Staffeld, A. Baro, F. Giesselmann, S. Laschat, *Chem. Rev.* **2016**, *116*, 1139–1241; b) *Handbook of Liquid Crystals* 2nd ed. (Eds.: J. Goodby, P. J. Collings, T. Kato, C. Tschierske, H. Gleeson, P. Raynes), Wiley-VCH, Weinheim, **2014**; c) B. M. Rosen, C. J. Wilson, D. A. Wilson, M. Peterca, M. R. Imam, V. Percec, *Chem. Rev.* **2009**, *109*, 6275–6540; d) T. Kato, J. Uchida, T. Ichikawa, T. Sakamoto, *Angew. Chem. Int. Ed.* **2018**, *57*, 4355–4371; *Angew. Chem.* **2018**, *130*, 4438–4455; e) R. J. Bushby, K. Kawata, *Liq. Cryst.* **2011**, *38*, 1415–1426.
[2] a) T. Kato, M. Yoshio, T. Ichikawa, B. Soberats, H. Ohno, M. Funahashi, *Nat. Rev. Mater.* **2017**, *2*, 17001–17021; b) S. Sergeyev, W. Pisula, Y. H. Geerts, *Chem. Soc. Rev.* **2007**, *36*, 1902–1929; c) M. O'Neill, S. M. Kelly, *Adv. Mater.* **2011**, *23*, 566–584; d) L. Schmidt-Mende, A. Fechtenkötter, K. Müllen, E. Moons, R. H. Friend, J. D. MacKenzie, *Science* **2001**, *293*, 1119–1122; e) M. Funahashi, *Polym. J.* **2017**, *49*, 75–83; f) S. Laschat, A. Baro, N. Steinke, F. Giesselmann, C. Hägele, G. Scalia, R. Judele, E. Kapatsina, S. Sauer, A. Schreivogel, M. Tosoni, *Angew. Chem. Int. Ed.* **2007**, *46*, 4832–4887; *Angew. Chem.* **2007**, *119*, 4916–4973; g) X. Feng, V. Marcon, W. Pisula, M. R. Hansen, J. Kirkpatrick, F. Grozema, D. Andrienko, K. Kremer, K. Müllen, *Nat. Mater.* **2009**, *8*, 421–426.
[3] a) B. N. Boden, R. J. Bushby, J. Clements, M. V. Jesudason, P. F. Knowles, G. Williams, *Chem. Phys. Lett.* **1988**, *152*, 94–99; b) D. Adam, F. Closs, T. Frey, D. Funhoff, D. Haarer, P. Schuhmacher, K. Siemensmeyer, *Phys. Rev. Lett.* **1993**, *70*, 457–460; c) D. Adam, P. Schuhmacher, J. Simmerer, L. Häussling, K. Siemensmeyer, K. H. Etzbachi, H. Ringsdorf, D. Haarer, *Nature* **1994**, *371*, 141–143.
[4] a) Y. Sagara, T. Kato, *Nat. Chem.* **2009**, *1*, 605–610; b) Y. Sagara, S. Yamane, M. Mitani, C. Weder, T. Kato, *Adv. Mater.* **2016**, *28*, 1073–1095; c) T. Kato, M. Gupta, D. Yamaguchi, K. P. Gan, M. Nakayama, *Bull. Chem. Soc. Jpn.* **2021**, *94*, 357–376; d) S. Yagai, S. Okamura, Y. Nakano, M. Yamauchi, K. Kishikawa, T. Karatsu, A. Kitamura, A. Ueno, D. Kuzuhara, H. Yamada, T. Seki, H. Ito, *Nat. Commun.* **2014**, *5*, 4013; e) V. N. Kozhevnikov, B. Donnio, D. W. Bruce, *Angew. Chem. Int. Ed.* **2008**, *47*, 6286–6289; *Angew. Chem.* **2008**, *120*, 6382–6385.
[5] a) M. Lehmann, M. Dechant, M. Lambov, T. Ghosh, *Acc. Chem. Res.* **2019**, *52*, 1653–1664; b) E. J. Foster, R. B. Jones, C. Lavigueur, V. E. Williams, *J. Am. Chem. Soc.* **2006**, *128*, 8569–8574; c) E. Beltrán, J. L. Serrano, T. Sierra, R. Giménez, *J. Mater. Chem.* **2012**, *22*, 7797–7805; d) G. Kestemont, V. D. Halleux, M. Lehmann, D. A. Ivanov, M. Watson, Y. Henri Geerts, *Chem. Commun.* **2001**, 2074–2075; e) C. Tschierske, *Angew. Chem. Int. Ed.* **2013**, *52*, 8828–8878; *Angew. Chem.* **2013**, *125*, 8992–9047; f) C. Hägele, E. Wuckert, S. Laschat, F. Giesselmann, *ChemPhysChem* **2009**, *10*, 1291–1298; g) P. Staffeld, M. Kaller, S. J. Beardsworth, K. Tremel, S. Ludwigs, S. Laschat, F. Giesselmann, *J. Mater. Chem. C* **2013**, *1*, 892–901.
[6] a) D. Gonzalez-Rodriguez, A. P. H. J. Schenning, *Chem. Mater.* **2011**, *23*, 310–325; b) I. Paraschiv, K. de Lange, M. Giesbers, B. van Lagen, F. C. Grozema, R. D. Abellon, L. D. A. Siebbeles, E. J. R. Sudhölter, H. Zuilhof, A. T. M. Marcelis, *J. Mater. Chem.* **2008**, *18*, 5475–5481; c) J. Miao, L. Zhu, *Chem. Mater.* **2010**, *22*, 197–206; d) J. A. Duro, G. de la Torre, J. Barberá, J. L. Serrano, T. Torres, *Chem. Mater.* **1996**, *8*, 1061–1066.
[7] A. Demenev, S. H. Eichhorn, T. Taerum, D. F. Perepichka, S. Patwardhan, F. C. Grozema, L. D. A. Siebbeles, R. Klenkler, *Chem. Mater.* **2010**, *22*, 1420–1428.
[8] a) Y. Sagara, S. Yamane, T. Mutai, K. Araki, T. Kato, *Adv. Funct. Mater.* **2009**, *19*, 1869–1875; b) Y. Sagara, T. Kato, *Angew. Chem. Int. Ed.* **2011**, *50*, 9128–9132; *Angew. Chem.* **2011**, *123*, 9294–9298; c) S. Yamane, Y. Sagara, T. Kato, *Chem. Commun.* **2013**, *49*, 3839–3841; d) S. Yamane, Y. Sagara, T. Mutai, K. Araki, T. Kato, *J. Mater. Chem. C* **2013**, *1*, 2648–2656.
[9] a) B. Soberats, M. Hecht, F. Würthner, *Angew. Chem. Int. Ed.* **2017**, *56*, 10771–10774; *Angew. Chem.* **2017**, *129*, 10911–10914; b) S. Herbst, B. Soberats, P. Leowanawat, M. Stolte, M. Lehmann, F. Würthner, *Nat. Commun.* **2018**, *9*, 2646–2655; c) M. Hecht, B. Soberats, J. Zhu, V. Stepanenko, S. Agarwal, A. Greiner, F. Würthner, *Nanoscale Horiz.* **2019**, *4*, 169–174.
[10] F. García, J. Buendía, S. Ghosh, A. Ajayaghosh, L. Sánchez, *Chem. Commun.* **2013**, *49*, 9278–9280.
[11] a) E. E. Greciano, L. Sánchez, *Chem. Eur. J.* **2016**, *22*, 13724–13730; b) E. E. Greciano, B. Matarranz, L. Sánchez, *Angew. Chem. Int. Ed.* **2018**, *57*, 4697–4701; *Angew. Chem.* **2018**, *130*, 4787–4791; c) E. E. Greciano, R. Rodríguez, K. Maeda, L. Sánchez, *Chem. Commun.* **2020**, *56*, 2244–2247; d) E. E. Greciano, S. Alsina, G. Ghosh, G. Fernández, L. Sánchez, *Small Methods* **2020**, *4*, 1900715.
[12] a) F. Würthner, C. R. Saha-Möller, B. Fimmel, S. Ogi, P. Leowanawat, D. Schmidt, *Chem. Rev.* **2016**, *116*, 962–1052; b) R. K. Gupta, A. A. Sudhakar, *Langmuir* **2019**, *35*, 2455–2479; c) F. Würthner, C. Thalacker, S. Diele, C. Tschierske, *Chem. Eur. J.* **2001**, *7*, 2245–2253.
[13] a) R. K. Gupta, S. K. Pathak, B. Pradhan, M. Gupta, S. K. Pal, A. A. Sudhakar, *ChemPhysChem* **2016**, *17*, 859–872; b) R. K. Gupta, D. Das, M. Gupta, S. K. Pal, P. K. Iyer, A. S. Achalkumar, *J. Mater. Chem. C* **2017**, *5*, 1767–1781.
[14] J. Buendía, J. Calbo, E. Ortí, L. Sánchez, *Small* **2017**, *13*, 1603880.
[15] F. García, L. Sánchez, *J. Am. Chem. Soc.* **2012**, *134*, 734–742.
[16] A. Seki, M. Yoshio, *ChemPhysChem* **2020**, *21*, 328–334.
[17] E. Li, K. Jie, M. Liu, X. Sheng, W. Zhu, F. Huang, *Chem. Soc. Rev.* **2020**, *49*, 1517–1544.
[18] X. Hao, B. Xiong, M. Ni, B. Tang, Y. Ma, H. Peng, X. Zhou, I. I. Smalyukh, X. Xie, *ACS Appl. Mater. Interfaces* **2020**, *12*, 53058–53066.

Chem. Eur. J. **2021**, *27*, 14282–14286   www.chemeurj.org

14286   © 2021 The Authors. Chemistry - A European Journal published by Wiley-VCH GmbH